GEOPHYSICAL RESEARCH LETTERS, VOL. 23, NO. 9, PAGES 917-920, MAY 1, 1996

The $M_W = 8.1$ Antofagasta (North Chile) Earthquake of July 30, 1995: First results from teleseismic and geodetic data

J.C. Ruegg[1,2], J. Campos[3], R. Armijo[1], S. Barrientos[3], P. Briole[1,2], R. Thiele[3], M. Arancibia[4], J. Cañuta[4], T. Duquesnoy[5], M. Chang[6], D. Lazo[7], H. Lyon-Caen[1,2], L. Ortlieb[8], J.C. Rossignol[1], and L. Serrurier[7]

Abstract. A strong (M_W = 8.1) subduction earthquake occurred on July 30, 1995 in Antofagasta (northern Chile). This is one of the largest events during this century in the region. It ruptured the southernmost portion of a seismic gap between 18°S and 25°S. In 1992 we had used GPS to survey a network with about 50 benchmarks covering a region nearly 500 km long (N-S) and 200 km wide (E-W). Part of these marks were re-surveyed with GPS after the 1995 earthquake. Comparison with 1992 positions indicate relative horizontal displacement towards the trench reaching 0.7 m. The inland subsided several decimeters. The Mejillones Peninsula was uplifted by more than 15 cm. Teleseismic body-wave modelling of VBB records gives a subduction focal mechanism and source time function with three distinct episodes of moment release and southward directivity. Modelling the displacement field using a dislocation with uniform slip in elastic half-space suggests a rupture zone with 19°-24° eastward dip extending to a depth no greater than 50 km with N-S length of 180 km and an average slip of about 5 m. The component of right-lateral slip inferred both from the teleseismic and geodetic data does not require slip partitioning at the plate boundary. That the well-constrained northern end of the 1995 rupture zone lies under the southern part of the Mejillones Peninsula increases the probability for a next rupture in the gap north of it.

Introduction

Coastal southern Peru and northern Chile have been identified as seismic gaps with high potential for large earthquakes in the near future [*Nishenko,* 1985]. A sequence of two great subduction earthquakes (M = 8.5-9) ruptured contiguous fault segments each about 450 km long in 1868 (southern Peru) and 1877 (northern Chile). The recurrence period of earthquakes M>8 in the region is of the order of 100 years [*Comte and Pardo,* 1991].

Since 1991 we have developed a French-Chilean project for the study of the seismic cycle and of precursory deformation in Northern Chile [*Armijo et al.,* 1993]. The project includes regional tectonics, a geophysical observatory in the center of the gap near Iquique, and repeated geodetic surveys of a GPS network first measured with dual-frequency receivers in 1991-1992 (Fig. 1). There are more than 50 benchmarks tied to average sea-level at three tide gages. The GPS network covers both the segment that ruptured in 1877 (Arica to Mejillones Peninsula; 18°S-23°S) and part of the smaller gap between Mejillones Peninsula and Taltal (roughly between 23°S-26°S) in which no large (M>8) historical earthquakes have been reported. South of our survey, the segment roughly between 26°S-29.5°S ruptured in 1922 (M_W = 8.4) [*Kelleher,* 1972].

The July 30, 1995, a M_W = 8.1, earthquake ruptured the southernmost part of the surveyed area, with hypocenter determined by the local network to be at 23.43°S; 70.48°W and 36 km depth [*Monfret et al.,* 1995] (Fig. 1). Two weeks after the event we remeasured part of the GPS network. Here we use the preliminary results on geodetic displacements and long-period teleseismic recordings to infer the location, geometry and dynamics of the rupture through simple modelling.

Teleseismic modelling of the mainshock

The location of the 1995 earthquake below Mejillones peninsula [*Monfret et al.,* 1995] falls in the northern part of the area of aftershock epicenters determined by the USGS, which extends about 220 km parallel to the Chilean coast (Fig. 1). Although the USGS magnitude M_S is 7.3, the Harvard's CMT solution yields $M_0 = 1.7 \times 10^{21}$ Nm. The corresponding fault plane solution and aftershock distribution are consistent with east-dipping thrusting on the subduction interface.

We used Very Broad Band (VBB) teleseismic digital records from the IRIS and GEOSCOPE networks. Only mantle body waves from stations at distances of 30° < D_P <90°, and 34°< D_{SH} <87° were included in the data set, to avoid upper mantle and core arrivals (Fig. 2). We used the inversion procedure of *Nábelek* [1984] in simple half-space model to estimate the source parameters and performed a limited exploration of parameter space, following the strategy of *Campos et al.* [1994]. To control the resolution of the inversion and to determine rupture propagation and subevent distribution, we proceeded by steps with increasing model complexity. We equalized the records to displacement seismograms with the same gain at a distance of 40° from the epicenter and filtered them with a bandpass filter between 0.01 and 0.5 Hz.

As a first step, we determined the best point-source model at the hypocenter. With linearized inversion, we obtained a solution with N8°E strike, 19° dip, and 110° rake. The centroid source depth is 32 km with seismic moment of 9.0×10^{20} Nm, which is about half of the CMT moment. Inversion was repeated for a point-source model with a uniformly propagating rupture using the above focal mechanism. Directivity obtained

[1]Institut de Physique du Globe, Paris, France
[2]CNRS, France
[3]Universidad de Chile, Santiago, Chile
[4]SERNAGEOMIN, Santiago, Chile
[5]IGN, Saint Mandé, France
[6]IGP, Lima, Peru
[7]Universidad Arturo Prat, Iquique, Chile
[8]ORSTOM, Paris, France

Paper number 96GL01026
0094-8534/96/96GL-01026$05.00

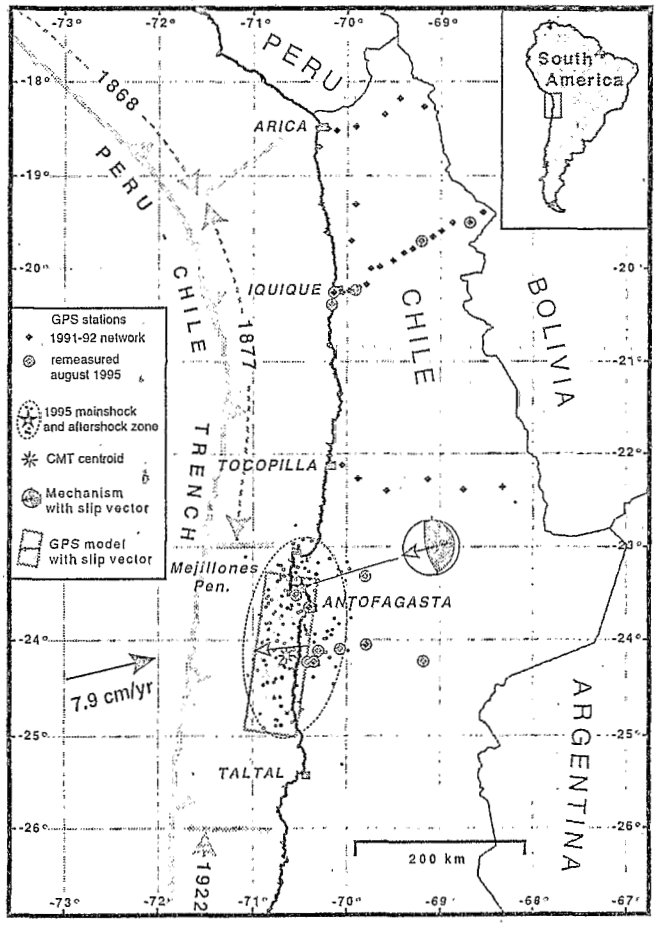

Figure 1. Subduction segments and seismic gaps in Northern Chile: GPS network, aftershocks and models for the 1995 Antofagasta earthquake. Plate convergence (7.9 cm/yr) from De Mets et al. [1990].

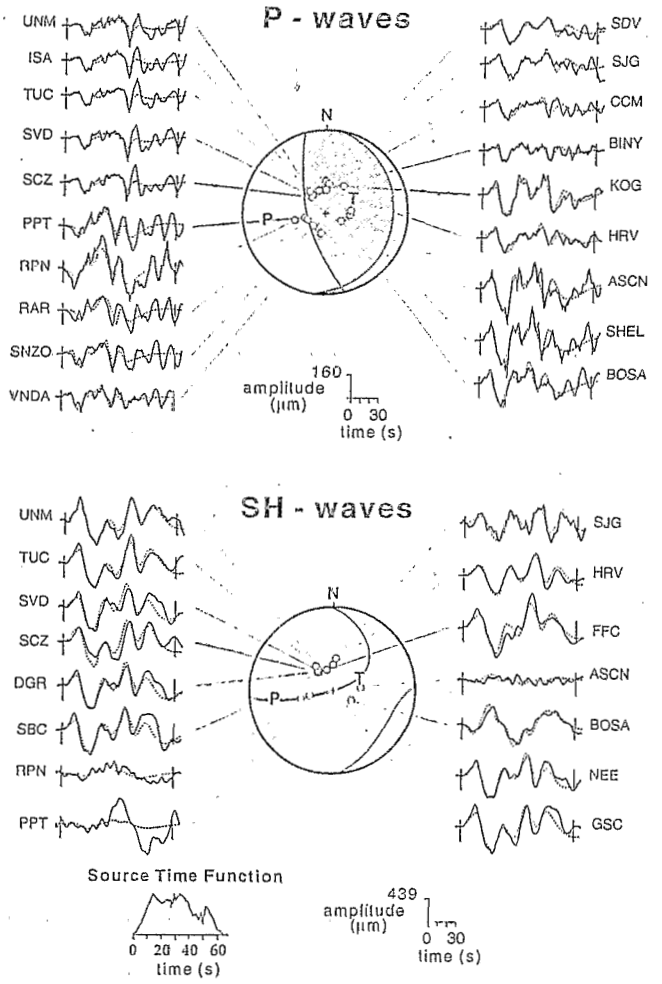

Figure 2. Average fault plane solution for the three point source model (Table 1) and and corresponding observed and synthetic body-wave band-pass filtered displacement.

is southward with average rupture velocity of 3.3 km s^{-1} (85% of the S-wave velocity). Directivity is clear on the P-wave records (Fig. 2); stations south of the epicenter record shorter periods than stations north of it.

As a second step, we inverted for average moment release with fixed fault geometry and found a source-time function with three distinct episodes of moment release (Fig. 2). Then, fixing the first source at the hypocenter (23.43°S; 70.48°W), we inverted for depth, fault mechanism, moment release, and the location of the second and third sources. Then we globally inverted for all parameters of the three point sources obtaining the same total moment and average mechanism as for the best single point source model (Table 1).

GPS data and modelling

Our GPS network comprises 4 profiles 150 km apart running between the coast and the Altiplano (Fig. 1). Points along the coast every 50 km ensure good resolution where maximum deformation is expected. Position coordinates for the 1992 campaign were estimated with daily solutions using the GAMIT software [*Bock et al.*, 1986] and precise IGS orbital parameters. Long vectors were estimated between Iquique, Antofagasta, and 3 permanent IGS stations. The repeatability on each individual baseline is less than 15 mm and the overall rms residuals of the adjustment is 19 mm.

Fifteen days after the 1995 earthquake, we remeasured part of the GPS network in the epicentral area and in the central part of the gap (Iquique). For this preliminary study, the 1995 measurements were analyzed with the GPPS software (simpler but less accurate than GAMIT) using precise IGS orbits. A set of new relative coordinates were obtained for the 10 points in the area of the 1995 shock using the position of point PA6 in 1992-as-reference (Fig. 3). The repeatability is better than 30 mm on each individual baseline, and the overall rms residuals of the adjustment is about 22 mm.

Comparison with the 1992 coordinates gives relative displacement with maximum combined error (2σ) of ±4 cm (Fig. 3, Table 2). This error, however, does not consider possible systematic bias induced by an heterogeneous troposphere, for

Table 1. Source parameters from body-wave modelling

Source	Mo	A	B	H	Az	T
1	4.1	7/22/110	165/70/82	35	-	0
2	3.9	9/16/113	165/75/84	33	187	25
3	0.9	8/18/110	167/73/84	31	190	50

Moment (Mo) in 10^{20} N m. Strike/dip/rake for primary (A) and auxiliary (B) planes in degrees. Depth (H) in km. Azimuth (Az) and delay (T) from first source in degrees and seconds.

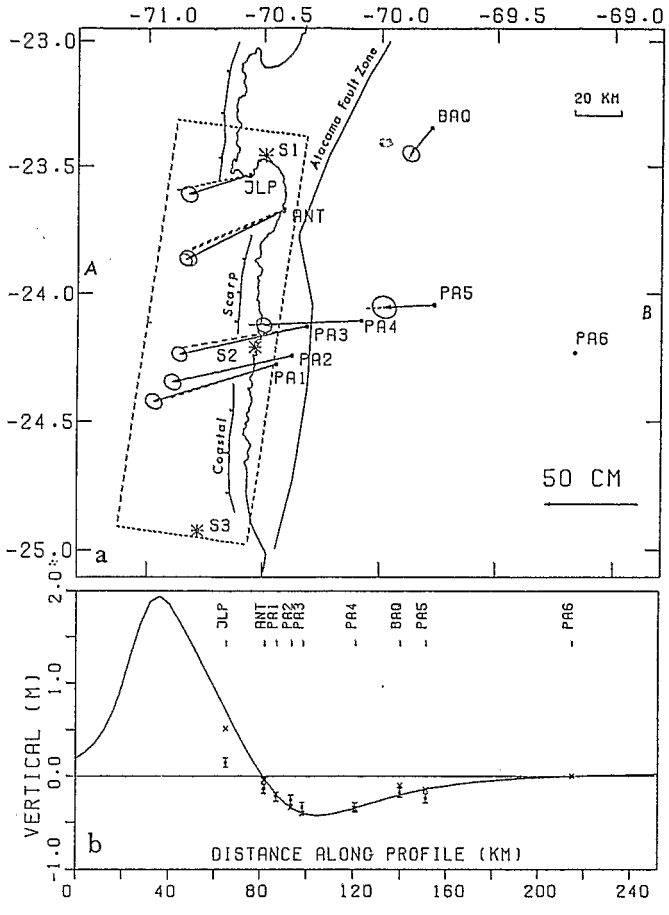

Figure 3. Uniform slip model based on GPS measurements. Observed and modelled values from Table 2. (a) Fit to horizontal displacement with 19° dip (solid arrow with 95% confidence ellipses, observed; dashed, modelled). S1, S2, S3 are the 3 point sources of Table 1. (b) Fit to vertical displacement with 24° dip (squares with error bars, observed; crosses, modelled; curve, modelled across AB section).

which the vertical component is especially sensitive. The relative horizontal displacement reaches a maximum of about 70 cm, and strikes ENE-WSW. Although resolved with less accuracy, the vertical displacement relative to PA6 is mostly subsidence, with a maximum of 34 cm, except for the point in the southern end of the Mejillones Peninsula (JLP), which shows a relative uplift of 15 cm.

To model the coseismic surface displacement field we use a dislocation embedded in an elastic half space [*Okada,* 1985]. The earthquake fault is taken as a rectangular plane with N8°E strike consistent with the fault plane solution obtained from body-wave inversion, and it is positioned less than 2 km distant from the hypocenter. By trial and error we obtained a satisfactory fit to the displacement vectors with eastward dip between 19° and 24° consistent with that of the subduction interface deduced from seismicity [*Comte et al.,* 1994] and with the fault plane solution. The uniform slip required is of about 5 m due N265°E (4.5 m thrust; 1 m right-lateral slip). This implies about 1 m of maximum absolute horizontal displacement at point PA3 (Table 2). The northern end of the rupture at 23.3°S under Mejillones Peninsula is well constrained by the fit to the vectors at and north of Antofagasta (Fig. 3a). The width (60 km) and the length (180 km) of the rupture are compatible with the aftershock distribution and with a maximum depth of 50 km for the seismically coupled interface [*Tichelaar and Ruff,* 1991]. Taking shear modulus of 33 GPa this gives a seismic moment of 1.5 x 10^{21} Nm, the same as the Harvard's CMT solution. The rupture, however, does not extend to the northern end of the aftershock zone and does not appear to reach the ocean floor (Fig. 1).

Our first-order model overestimates the vertical displacement of points near the coast (Fig. 3b). However, the uncertainty in the vertical component of the GPS vectors for these points is probably greater than our statistical estimate due to tropospheric contrast between the wet coast and the desertic inland plateau (at 1000 m average elevation). To refine the interpretation of vertical displacement and better constrain the fault geometry the 1995 and 1992 measurements need to be processed with the same software and to be calibrated with respect to distant stations of the IGS network. Calibration must also include some external constraints. For instance, preliminary inspection of the tide-gage record at Antofagasta shows no significant coseismic vertical variation (within a resolution of 5 cm). Besides, shoreline coseismic uplift was deduced from the observation of dead algae along the coast [*Ortlieb et al.,* 1995]. This suggests uplift that reaches a maximum of about 40 cm at the southern end of the Mejillones Peninsula, and of a few cm at Antofagasta, in agreement with the gradient of vertical displacement in the model (Fig. 3b). It is crucial to precisely determine the absolute vertical displacement to resolve further the total deformation in the 1992-1995 period, whether it is all coseismic or not.

Discussion

Both the GPS and body-wave models require a fault strike parallel to the trench and a slip vector directed WSW, consistent within few degrees with the relative plate convergence (Fig. 1). This implies oblique slip with 20-25% right-lateral motion at the subduction interface; an argument against slip partitioning in this part of the plate boundary. *Armijo and Thiele* [1990] described left-lateral morphological offsets along the trench-parallel Atacama Fault system (Fig. 3) suggesting no room for slip partitioning. The modelled fault plane with 24° dip requires the subduction interface to shallow toward the west to reach the ocean floor at the trench. This change in dip would induce extensional strain near the surface consistent with the Quaternary deformation described on the Mejillones

Table 2. Observed and modelled displacement

Station	GPS (1992-1995)			Modelled		
PA1	-66	-20	-22	-57	-15	-38
PA2	-64	-14	-26	-63	-10	-51
PA3	-69	-15	-34	-68	-08	-55
PA4	-52	-02	-34	-64	01	-41
PA5	-27	01	-24	-37	02	-15
PA6	0	0	0	0	0	0
ANT	-53	-26	-13	-50	-17	-23
AN0	-53	-27	-14	-50	-17	-22
JLP	-33	-10	15	-40	-04	34
BAQ	-12	-14	-18	-14	-15	-11

Components relative to PA6 (East, North, vertical, in cm). Adding modelled absolute displacement for PA6 (-[29, 2, 3] cm) yields absolute displacement.

Peninsula by *Armijo and Thiele* [1990]. They suggested that such a subduction interface geometry may have caused large-scale west-dipping normal faulting in the fore-arc which would be responsible of the formation of the prominent Coastal Scarp of Northern Chile (Fig. 3).

The Antofagasta earthquake raises some puzzling problems. Despite its large moment, the associated tsunami recorded at the Antofagasta tide-gage (wave 1.3 m high), the magnitude M_S (7.3), the maximum felt intensity (VII) and the destruction were moderate. This casts doubt on the evaluation of the former regional seismicity, both old instrumental and historical. Events similar to the 1995 one may be underestimated, or ignored. The small Ms/Mw ratio can be explained by the presence of two peaks in the displacement spectra at 65 and 130 s. Our body wave modelling includes the 65 s peak only, due to the low-frequency band-pass filtering. The discrepancies between seismic moments determined with body waves and geodetic data is also consistent with moment release at low frequency. Preliminary inspection of our VBB record at Iquique shows a slow (low-frequency) start of the rupture process. Both the low-frequency peak and the start hint at peculiar rupture dynamics including a slow earthquake.

Despite the large surface displacement observed with GPS no significant surface break was observed along the numerous Quaternary faults described in the epicentral area [*Armijo and Thiele,* 1990]. However, the occurrence of ground fissures along two faults segments (Cerro Moreno and Salar del Carmen) could have resulted from slip on those faults at some depth, possibly due to small aftershocks. The GPS model implies coseismic subsidence of the high coastal range and uplift of offshore areas. Interseismic vertical deformation possibly by postseismic relaxation in the opposite sense will probably be accomodated by normal faulting at the Coastal Scarp.

The place of the 1995 earthquake in the seismic cycle is unclear. Although it ruptured most of the 23°S-26°S gap between the 1877 and the 1922 rupture zones (Fig. 1), two interplate thrust events of moderate magnitude have apparently ruptured parts of this gap [*e.g., Tichelaar and Ruff,* 1991]: (a) on 12/28/1966 (M_W=7.4), with aftershock zone between 25°S-25.7°S and (b) on 3/5/1987 (M_W=7.3), with aftershock zone 24°S-24.7°S and a local tsunami. The 1995 rupture zone overlaps that of the 1987 event but does not reach that of 1966. In addition, *Kausel and Campos* [1992] interpreted the 1950 (M_S=8) extensional event at 100 km depth within the subducted slab, east of Antofagasta, to indicate increased potential for strong earthquakes at the plate interface.

The 1995 earthquake apparently did not rupture under the northern Mejillones Peninsula, thus not reaching the segment supposed to have broken in 1877. This is in spite of nucleation that occurs at the northern end of the 1995 rupture. Hence the subduction interface under Mejillones Peninsula, which seems to have acted as a barrier to southward propagation in 1877, has now been both an asperity from which the 1995 event propagated southward, and again a barrier to northward propagation. This suggests that the potential for a large earthquake in the gap north of Antofagasta is now increased.

Acknowledgements. This is part of a cooperative project between Universidad de Chile, Sernageomin, Universidad A. Prat and the French Institut National des Sciences de l'Univers-CNRS. It was supported by INSU programs Tectoscope-Positionnement and PNRN, by the French Ministère des Affaires Etrangères (comité ECOS), and by the IPGP. We thank all those who helped with the field work, particularly I. Cifuentes, V. Farra, L. Banchero, A. Matrás, and L. Uribe. We thank local authorities for logistical support, especially J.C. Parra, J. Amaya, and A. Tello. A. Deschamps and K. Feigl made constructive reviews. Contribution IPGP N° 1407.

References

Armijo R. and R. Thiele, Active faulting in Northern Chile: Ramp stacking and lateral decoupling along a subduction plate boundary, *Earth Planet. Sci. Lett., 98*, 40-61, 1990.

Armijo R. et al., Crustal deformation and seismic cycle in Northern Chile, *Seism. Res. Lett., 94*, 24, 1993.

Bock, Y. et al., Interferometric analysis of GPS phase observations, *Manuscr. Geod., 11*, 282-288, 1986.

Campos, J. et al., Faulting process of the 1990 June 20 Iran earthquake from broad-band records, *Geophys. J. Int., 118*, 31-46, 1994.

Comte, D. and M. Pardo, Reappraisal of great historical earthquakes in the Northern Chile and southern Peru seismic gaps, *Natural Hazards, 4*, 23-44, 1991.

Comte, D. et al., Determination of seismogenic interplate contact zone and crustal seismicity around Antofagasta, northern Chile using local data, *Geophys. J. Int., 116*, 553-561, 1994.

DeMets, C., R.G. Gordon, D.F. Argus and S. Stein, Current plate motions, *Geophys. J. Int., 101*, 425-478, 1990.

Kausel, E. and J. Campos, The Ms=8 tensional earthquake of December 1950 of northern Chile and its relation to the seismic potential of the region, *Phys. Earth Planet. Int., 72*, 220-235, 1992.

Kelleher J., Rupture zones of large south American earthquakes and some predictions, *J. Geophys. Res., 77*, 2087-2103, 1972.

Monfret T. et al., The July 30, 1995 Antofagasta earthquake: an "hypocritical" seismic event, *EOS Trans. AGU, 76 (46)*, 427, 1995.

Nábelek J.L., Determination of earthquake source parameters from inversion of body waves, Ph.D. thesis, 346 pp., Mass. Inst. of Technol. Cambridge, 1984.

Nishenko, S.P., Seismic potential for large and great intraplate earthquakes along the Chilean and southern Peruvian margins of South America: A quantitative reappraisal, *J. Geophys. Res., 90*, 3589-3615, 1985.

Okada Y, Surface deformation to shear and tensile faults in a half space, *Bull. Seism. Assoc. Am., 75*, 1135-1154, 1985.

Ortlieb, L. et al., Coseismic uplift motion near Antofagasta, N Chile, related to the July 30, 1995, Ms=7.3 event: first field evidence from the intertidal area, *EOS Trans. AGU, 76 (46)*, 375, 1995.

Tichelaar, B.W. and L.J. Ruff, Seismic coupling along the Chilean subduction zone, *J. Geophys. Res., 96*, 11997-12022, 1991.

J.C. Ruegg, URA 195 CNRS, R. Armijo, URA 1093 CNRS, Institut de Physique du Globe, 4, Place Jussieu, 75252 Paris, France. (e-mail: ruegg@ipgp.jussieu.fr; armijo@ipgp.jussieu.fr)

J. Campos, S. Barrientos, Universidad de Chile, Departamento de Geofísica, Blanco Encalada 2085, Santiago, Chile. (e-mail: campos@dgf.uchile.cl; sbarrien@dgf.uchile.cl)

(Received December 4, 1995; accepted March 21, 1996)